

Article

# Electrodeposition and Characterization of Poly 3-Amino-1,2,4-Triazole-5-Thiol Films on Brass Electrode in 0.1 M Methanol

Mohamed Damej <sup>1,2,\*</sup> , Mohammed Abouchane <sup>2</sup>, Mostafa Doubi <sup>1</sup>, Hamid Erramli <sup>1</sup>, Mohammed Benmessaoud <sup>1</sup> and Najat Hajjaji <sup>2</sup>

<sup>1</sup> Laboratory of Organic Chemistry Catalyst and Environment, Faculty of Sciences, Ibn Tofail University, P.O. Box 242, Kenitra 14000, Morocco

<sup>2</sup> Environment, Materials and Sustainable Development Team—CERNE2D, High School of Technology, Mohammed V University in Rabat, Kenitra 14000, Morocco

\* Correspondence: damejmohamed1979@gmail.com

**Abstract:** The electrochemical synthesis of conductive polymers (CPs) or semiconductors (SCs) is influenced by several parameters, such as the choice of monomers, solvents, support electrolytes, and the nature of dopants, which induce electrical conductivity in conjugated organic polymers. This work describes the electropolymerization of 3-amino-1,2,4-triazole-5-thiol (ATT) on a 60Cu-40Zn brass alloy. The synthesis of polymer film by electrochemical method was carried out by cyclic voltammetry and chronoamperometry in a medium of KOH 0.1 M dissolved in pure methanol CH<sub>3</sub>OH. The voltammograms obtained show that the ATT oxidizes anodically at a potential of 1.15 V. The effect of the sweep speed shows that the increase in the sweep speed is accompanied by the increase in the intensity of the first oxidation peak, indicating the acceleration of the process studied, and also indicating that the oxidation reaction of the monomers is essentially irreversible and controlled by a diffusion process. The polymer film analysis by electrochemical impedance spectroscopy shows a capacitive then diffusional behavior—this is a typical effect of conductive polymers. Analysis by EDX justifies the formation of a polymer film on the metal surface. This work was completed by theoretical calculation, which showed that the oxidation of the ATT considerably reduces the energy value of Gap  $E_{gap}$ , reaching a value of 2.07 eV—this shows that the polymer film is a semiconductive material.

**Keywords:** cyclic voltammetry; chronoamperometry; brass alloy; gap energy; semiconductor



**Citation:** Damej, M.; Abouchane, M.; Doubi, M.; Erramli, H.; Benmessaoud, M.; Hajjaji, N. Electrodeposition and Characterization of Poly 3-Amino-1,2,4-Triazole-5-Thiol Films on Brass Electrode in 0.1 M Methanol. *Coatings* **2022**, *12*, 1784. <https://doi.org/10.3390/coatings12111784>

Academic Editor: Aomar Hadjadj

Received: 31 August 2022

Accepted: 12 November 2022

Published: 21 November 2022

**Publisher's Note:** MDPI stays neutral with regard to jurisdictional claims in published maps and institutional affiliations.



**Copyright:** © 2022 by the authors. Licensee MDPI, Basel, Switzerland. This article is an open access article distributed under the terms and conditions of the Creative Commons Attribution (CC BY) license (<https://creativecommons.org/licenses/by/4.0/>).

## 1. Introduction

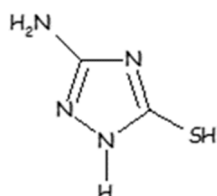
Copper and its alloys have interesting properties, such as electrical and thermal conductivity, and particularly good corrosion resistance, allowing them to be used in various industrial fields [1,2]. Much work has been done to study the formation of polymer films on metal substrates via by electrochemical methods in order to understand the mechanism of formation and growth of these polymer films [3–5]. Conductive or semiconductive polymer films have important electrical properties. Some of these films have been the subject of some industrial applications; for example, they can be used as a support for electronic components [6–9] and as a means of protection against corrosion by insulating polymer films [10–12]. The literature reports a number of studies on conductive polymers using aromatic systems such as thiophene [13], aniline [14,15], and fluorene [16]. The electropolymerization kinetics of 3-amino-1,2,4-triazole-5-thiole (ATT) on brass alloy was studied using cyclic voltammetry, chronoamperometry, electrochemical impedance techniques, and theoretical study; the metallic surface was analyzed using SEM/EDX. The polymer film was prepared by successive cycles of potential between 0 and 1.6 V. The oxidation reaction of the monomers is essentially irreversible and controlled by a diffusion process.

The electrochemical and theoretical study of synthesized polymer films shows that the latter is a semiconductor.

## 2. Experiment

### 2.1. Tested Monomer

The monomer used for the synthesis of the polymer films is called 3-amino-1,2,4-triazole-5-thiol (ATT). It is a commercial compound of the Flocka type (Scheme 1).



**Scheme 1.** Molecular structure of ATT.

### 2.2. Electropolymerization Electrolyte and Methods

The monomer oxidation was carried out in a solution of 0.1 M KOH dissolved in pure methanol.

Anodic oxidation was performed using the following two methods:

- Chronoamperometry: Polarization of a constant potential.
- Cyclic voltammetry: Cyclic scanning of the potential.

### 2.3. Brass Samples

The composition of the brass alloy studied was as follows (wt%): 60.61% Cu, 39.19% Zn, 0.12% Al, and 0.08% Si [17–19].

### 2.4. Electrochemical Cell

For all of the electrochemical tests, we used a conventional cell with three electrodes: a Ag-AgCl reference electrode, a large area platinum counter electrode, and an alloy working electrode 60Cu-40Zn. All experiments were performed in the supporting electrolyte CH<sub>3</sub>OH + 0.1 M KOH. Before use, the surface of the sample was polished with emery paper ranging from 600 to 2000, and then rinsed with distilled water.

### 2.5. Electrochemical Techniques

The cyclic voltammetry I-E, the chronoamperometry, and electrochemical impedance curves were performed using a potentiostat SP-200 Bio Logic type Science Instruments. The data were analyzed using the software Ec-Lab. Electrochemical impedance spectroscopy measurements were performed over a frequency range of 100 kHz to 10 mHz, with a signal amplitude disturbance of 1 mV·S<sup>-1</sup>. The data were presented in the form of Nyquist diagrams.

### 2.6. Energy Dispersion of X-ray

The EDX used is of brand PGT (Princeton Gamma-Tech, Princeton, NJ, USA) model Spirit, with a silicon diode-doped lithium type Prism 2000 (beryllium oxide window), with a resolution of 128 eV on the K-alpha of the Mn.

### 2.7. Theoretical Calculation

Quantum chemistry calculations were performed using Gaussian 09 software [20–22]. Geometric optimization of the different monomers was performed using DFT/B3LYP method with a base set of 6-31G (d, p) [23–26]. The gap energy  $E_{gap}$  was estimated using the equation below:

$$E_{gap} = E_{Lumo} - E_{Homo} \quad (1)$$

### 3. Results and Discussion

#### 3.1. Oxidation of 3-Amino-1,2,4-triazole-5-thiol (ATT)

##### 3.1.1. Poly-ATT Prepared by Cyclic Voltammetry

In the absence of monomer, the anodic electroactivity range was determined by the oxidation of the 0.1 M KOH support electrolyte. The voltammograms  $i = f(E)$  shown in Figure 1a were obtained by a cyclic sweep of the potential between 0 and 2.2 V with a sweep speed of  $10 \text{ mV}\cdot\text{s}^{-1}$ . In the presence of monomer, Figure 1b shows the voltammogram obtained during the formation of poly-3-amino-1,2,4-triazole-5-thiol (poly-ATT) on a brass alloy electrode by a potential cyclic sweep.

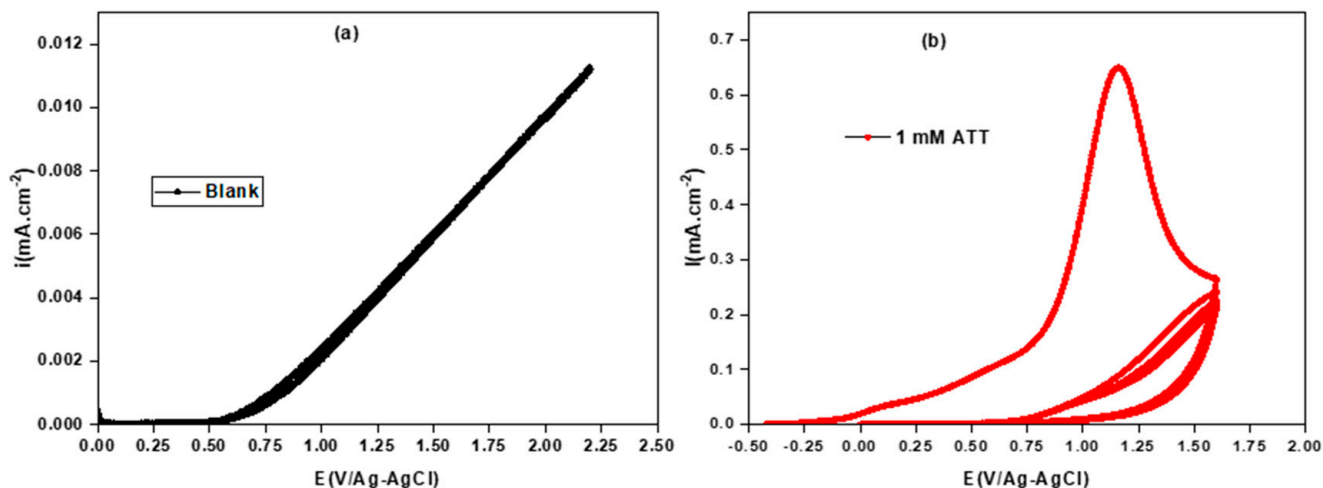


**Figure 1.** Voltammograms in the absence (a) and in the presence of monomer (b) on the electrode 60Cu-40Zn ( $[\text{ATT}] = 1 \text{ mM}$ ),  $dE/dt = 10 \text{ mV}\cdot\text{s}^{-1}$ .

The addition of monomer in the electrolytic medium indicates the appearance of a peak oxidation in the anodic domain (Figure 1b). This peak corresponds to the oxidation of ATT because it is absent in the control [12] (Figure 1a). However, no peak was detected during the cathodic scanning (return), showing that the species formed by oxidation of 3-amino-1,2,4-triazole-5-thiol are unstable free radicals. These radicals and their mesomer forms are coupled together to form a polymer deposit on the electrode surface. The anodic current peak appears at a potential of 1.15 V in the first cycle; from the second cycle, no peak is observed. The absence of a current peak during another potential sweep (go) can be explained by the formation of a homogeneous and compact film. At the end of the oxidation of the monomer, the current density stabilizes at a value of  $0.3 \text{ mA}\cdot\text{cm}^{-2}$ , which shows that the synthesized polymer film is semiconductive.

##### 3.1.2. Poly-ATT Prepared by Chronoamperometry

Chronoamperometry consists of following the evolution of the current as a function of time when the system is subjected to a fixed voltage. A constant potential of 1.15 V/Ag-AgCl was imposed on the working electrode for 30 min. The curve schematized by Figure 2, recorded during this operation, shows a constant current, suggesting the formation of a homogeneous and uniform film [10,12], but above all revealing that the formation of the film is controlled by the diffusion of the monomer towards the electrode surface.

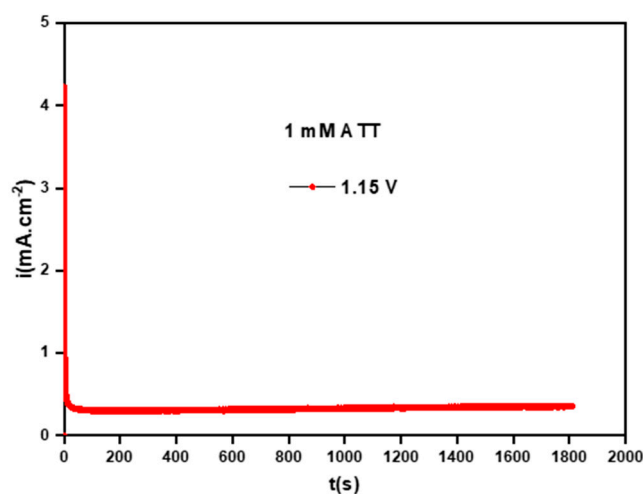


**Figure 2.** Chronoamperometry of a 1 mM ATT solution carried out at 1.15 V/Ag-AgCl on a brass alloy in pure methanol containing 0.1 M KOH.

At the end of the recording and after rinsing the active surface of the electrode, the brass alloy was placed in an electrochemical cell containing the electrolyte solution  $\text{CH}_3\text{OH} + 0.1 \text{ M KOH}$  without the addition of monomer (Figure 3).

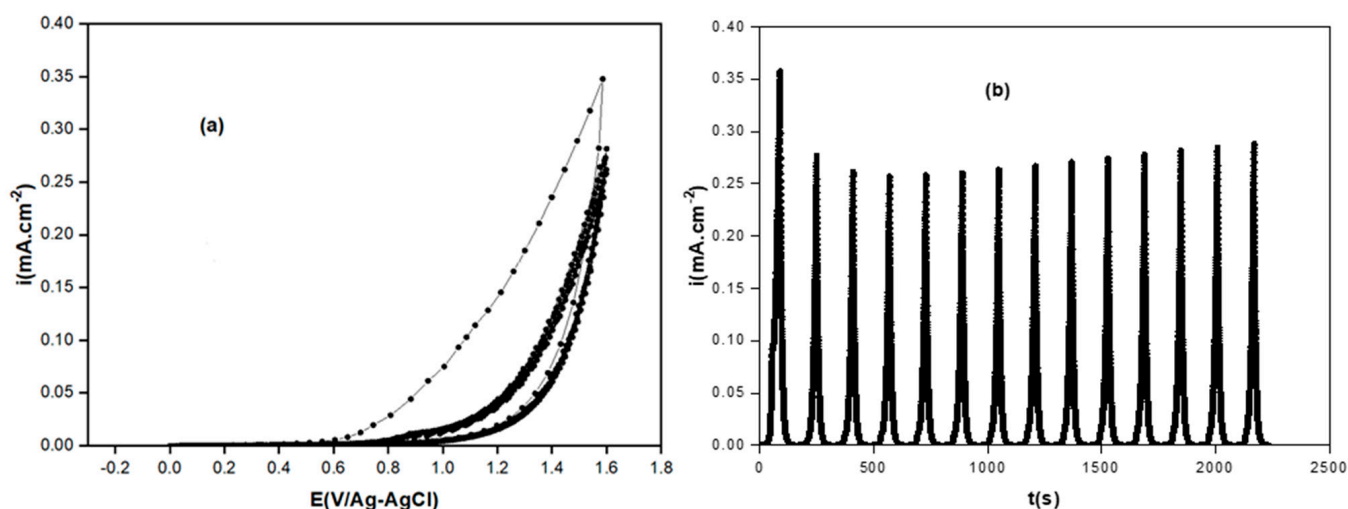


**Figure 3.** Electroactivity of poly-ATT recorded in pure methanol containing 0.1 M KOH,  $\nu = 10 \text{ mV}\cdot\text{s}^{-1}$ .

No peak was detected during the recording of voltammograms  $i = f(E)$  (Figure 3a), but the density of the current decreases and then begins to increase from the fourth cycle in a very regular way; this is more visible in Figure 3b, which illustrates the study of the electroactivity of the deposited film. This result may suggest that the material obtained activates the electrode because it has a structure allowing the penetration of counterion or any other inter-facial reaction.

### 3.2. Effect of Different Experimental Parameters

In this part, we will discuss the influence of different experimental parameters on the synthesis of poly-ATT, such as the applied potential, the pH of the solution, and the effect of the solvent.

### 3.2.1. Effect of the Applied Potential

To determine the applied potential effect on the nature of the polymer film synthesized, several experiments were carried out by modifying the applied potential. The chronoamperograms obtained by varying the potential between 0.70 V and 1.30 V/Ag-AgCl are shown in Figure 4.

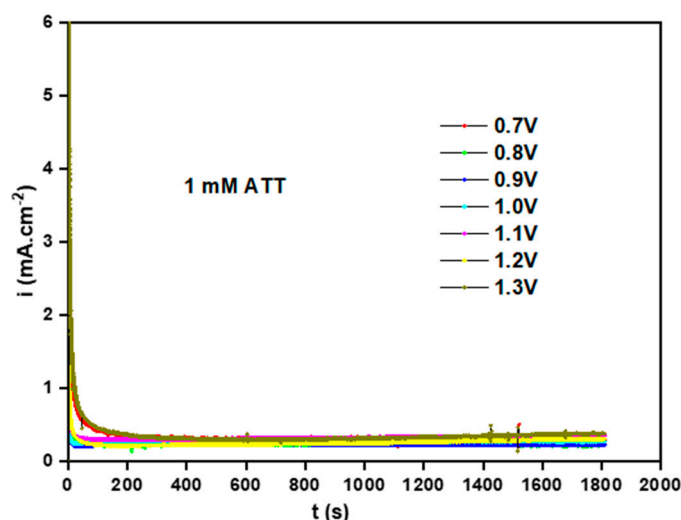


**Figure 4.** Chronoamperometry curves obtained at different potentials before and after the ATT oxidation peak potential.

The values of the initial and final current densities and of the anodic charge obtained for each applied potential are reported in Table 1.

**Table 1.** Values of the applied potentials and the initial and final current densities recorded respectively at ( $t_0 = 0.1$  s) and ( $t_f = 1800$  s) during the synthesis of poly-ATT on brass alloy in a methanolic solution 0.1 M KOH + 0.1 M ATT.

Synthesis of Poly-ATT			
E (V/Ag-AgCl)	$i_0$ (mA/cm <sup>-2</sup> )	$i_f$ (mA/cm <sup>-2</sup> )	Q (mC)
0.70	3.24	0.040	57.08
0.80	3.30	0.054	98.39
0.90	4.50	0.065	164.58
1.00	1.00	0.300	500.66
1.10	1.2	0.580	624.25
1.20	1.5	0.300	463.78
1.30	5.60	0.110	162.29

These results show that the ATT oxidation speed during the polymerization varies with the imposed potential; thus, for the potentials lower than 1 V and higher than 1.2 V, the poly-ATT films synthesized under these conditions are less conductive than those prepared at potentials between these two values. Indeed, electrolysis at a high potential ( $E \geq 1.2$  V) and at a potential  $E \leq 1$  V most often leads to the formation of cracked, porous films and low adhesions [27].

### 3.2.2. Effect of the pH of the Electrolyte Solution

After having studied the influence of the potential, we varied the pH of the electropolymerization solution between extreme values of 7.75 and 13 by varying the concentration of

KOH in order to specify the pH effect on the nature of the synthesized films of poly-ATT (Figure 5).

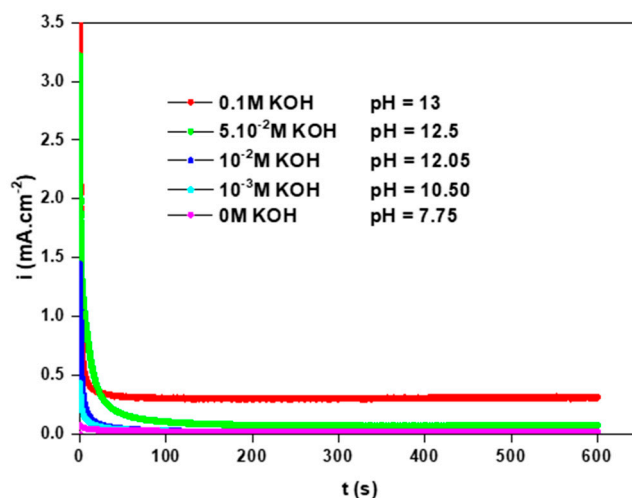


Figure 5. pH effect on synthesis by chronoamperometry of the poly-ATT.

The chronoamperograms obtained show that pH plays a primary role on the type of the synthesized polymer film. For concentrations less than 0.1 M KOH, the shape of the chronoamperometry curve shows that the current density decreases rapidly until a very low value tending towards zero, which indicates that the synthesized polymer film is an insulator.

### 3.2.3. Solvent Effect

The chronoamperometry study of ATT at a 1 mM concentration was carried out in three different mediums: methanol  $\text{CH}_3\text{OH}$ , acetonitrile  $\text{CH}_3\text{CN}$ , and dichloromethane  $\text{CH}_2\text{Cl}_2$  containing 0.1 M KOH as an electrolytic salt (Figure 6).

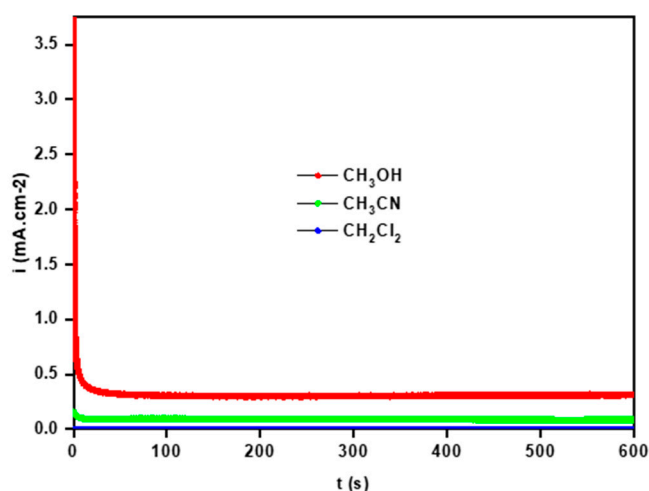


Figure 6. Chronoamperograms recorded in 60Cu-40Zn brass polarized at 1.15 V/Ag-AgCl in different solvents.

Chronoamperometry carried out in methanol or in acetonitrile leads to the formation of a polymer film on the surface electrode of a conductive nature. On the other hand, that formed in dichloromethane leads to an insulating film, which indicates that the electropolymerization medium has an effect on the nature of the synthesized polymer film.

### 3.3. Kinetic Study of Electropolymerization of Poly-ATT

Voltammograms obtained at different scanning speeds on a Cu-Zn (60/40) brass electrode in the electropolymerization solution are shown in Figure 7) and their characteristics are shown in Table 2.

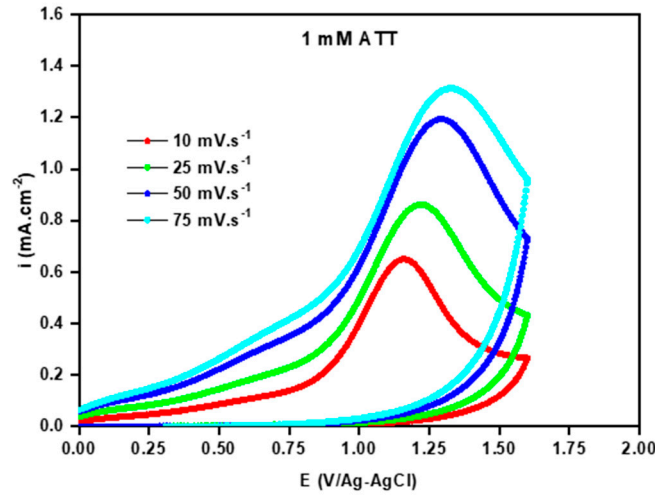


Figure 7. Oxidation-related voltammograms of ATT at different scan rates on 60Cu-Zn40 brass.

Table 2. Characteristics of voltamperograms obtained at the different scanning speeds.

Scanning Speed $\gamma$ ( $\text{mV}\cdot\text{s}^{-1}$ )	$i_{pic}$ ( $\text{mA}\cdot\text{cm}^{-2}$ )	$E_{pic}$ (V/Ag-AgCl)
10	0.656	1.156
25	0.867	1.213
50	1.192	1.293
75	1.314	1.329

The results obtained in Table 2 indicate that the oxidation peak intensity increases with increases in the scanning speed, which can be explained by the increase in the oxidation speed of the monomer (fast reaction). The curve plot  $i_{pic} = f(\gamma^{1/2})$  (Figure 8a) is a straight line through the origin, which confirms that the main reaction that leads to the polymer film formation is irreversible and controlled by diffusion [28,29].

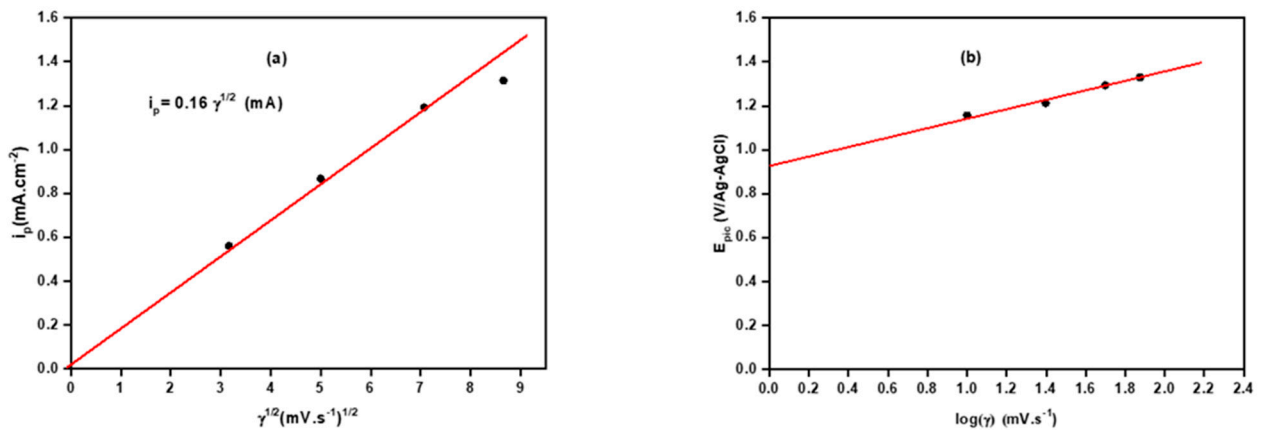


Figure 8. Peak current variation as a square root function of the scanning speed (a) and peak potential variation with the scanning speed logarithm (b).

The peak current related to the sweep speed is given by the following relationship:

$$i_p = 2.99 \times 10^5 \times n \times (\alpha \times n_a)^{1/2} \times A \times C_0 \times D_0^{1/2} \times \gamma^{1/2} \quad (2)$$

$$i_p = 0.227 \times n \times F \times A \times C_0 \times K_0 \times \exp\left(-\frac{\alpha \times n_a \times F}{R \times T} (E_p - E_0)\right) \quad (3)$$

where  $A$ ,  $D_0$ ,  $C_0$ ,  $n$ ,  $n_a$ ,  $\alpha$ ,  $K_0$ , and  $\gamma$  represent, respectively, the electrode surface, the diffusion coefficient, the concentration of the species that diffuses, the number of electrons exchanged, the apparent number of electrons transferred, the electronic transfer coefficient, the electronic transfer constant, and the scanning speed.

### 3.4. Electrochemical Impedance Spectroscopy

The impedance diagram was plotted at the abandonment potential in an alcoholic solution containing methanol + 0.1 M KOH after the formation of a poly-ATT polymer film by chronoamperometry for 30 min in the presence of 1 mM ATT. The Nyquist diagram of a frequency range varying from 10 mHz to 100 kHz is shown in Figure 9; the electrochemical parameters taken from this curve are recorded in Table 3.

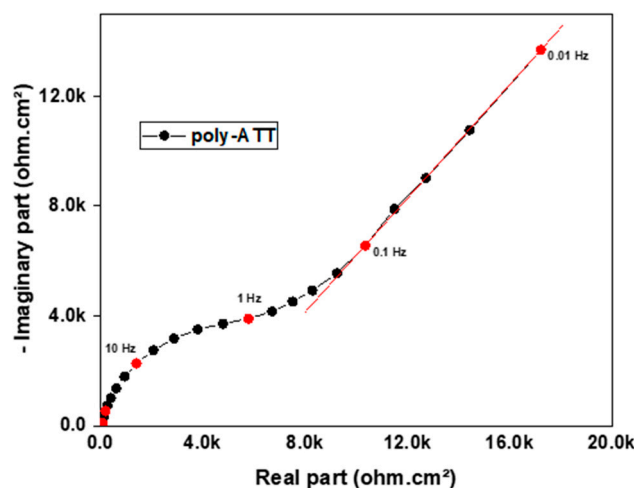


**Figure 9.** Nyquist diagram recorded with poly-ATT/60Cu-40Zn at abandonment potential in 0.1 M KOH/CH<sub>3</sub>OH.

**Table 3.** Electrochemical parameters obtained by the SIE of the interface 60Cu-40Zn/ poly-ATT in a medium 0.1 M KOH + CH<sub>3</sub>OH.

	$R_{ct}$ ( $k\Omega \cdot cm^2$ )	$C_{dl}$ ( $\mu F \cdot cm^{-2}$ )	N
Poly-ATT	10.2	31.2	0.5

The Nyquist representation can be divided into two regions: in the high frequency domain, a capacitive semi-circle is observed. This response has been attributed to charge transfer. In the low frequency domain, a linear variation of the impedance is observed, which corresponds to the Warburg impedance. This response is characteristic of a diffusion process within the working electrode; this capacitive then diffusional behavior is typical of semiconducting polymers [30,31].

Different models have been developed to explain the process obtained and to estimate the characteristic parameters of the phenomenon. The capacitive then diffusional impedance response can be represented by the following equivalent circuit [32] (Figure 10).

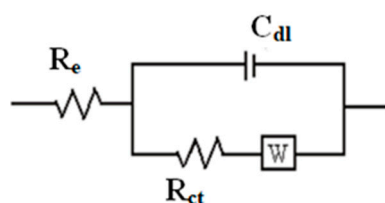


Figure 10. Equivalent electrical circuit.

### 3.5. Surface Analysis by EDX

The metal surface analysis by EDX after formation of a poly-ATT polymer film is shown in Figure 11.

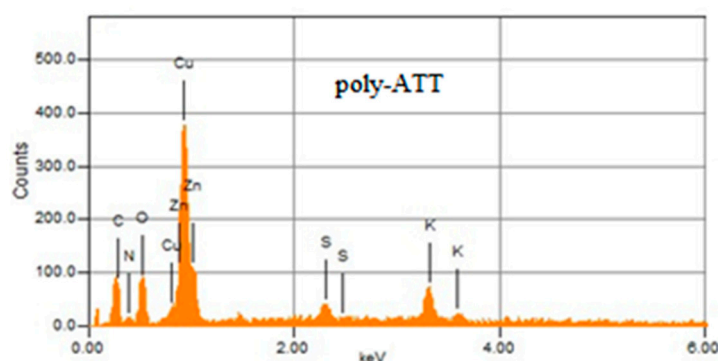


Figure 11. EDX spectrum obtained on the brass surface after synthesis of polymer film poly-ATT.

The EDX spectrum clearly shows the appearance of sulfur, carbon, and nitrogen on the electrode surface due to the presence of the organic molecule, which justifies the formation of a polymer film on the metallic surface.

### 3.6. Theoretical Study

The electronic structure of  $\pi$ -conjugated polymers can be described by a band structure. The highest energy occupied molecular orbital (HOMO) and the lower-energy unoccupied molecular orbital (LUMO) are the binding  $\pi$  and anti-binding  $\pi^*$  orbitals, respectively. Each new repeat pattern added leads to more and more levels with a decrease in the energy difference between HOMO and LUMO. A material is said to be insulating when the gap between its valence band and its conduction band is greater than 4 eV.

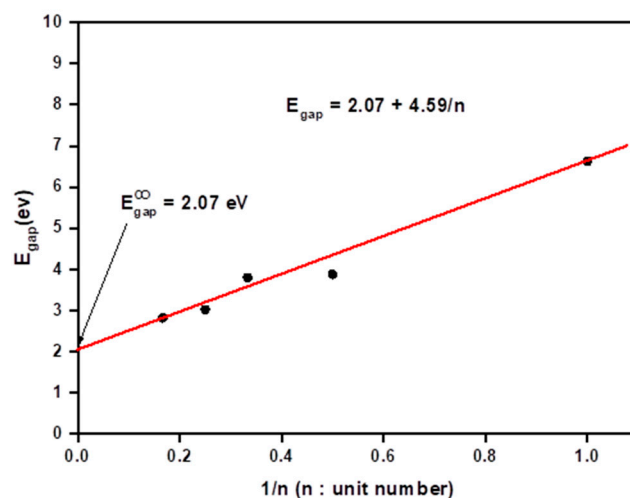
Theoretical calculation represents a very powerful tool to complete experimental studies, and therefore, to determine the nature of the polymer film synthesized, the different quantum parameters are summarized in Table 4.

Table 4. Quantum chemical parameters calculated for the different forms of monomer.

Unit Number	$E_{Lumo}$ (eV)	$E_{Homo}$ (eV)	$E_{gap}$ (eV)
1	3.2025	−3.0084	6.2109
2	−4.2169	−6.7732	2.5563
3	−3.5010	−6.5998	3.0988
4	−3.8468	−6.6790	2.8322
5	−4.4403	−6.8708	2.4305

The variation of the gap energy according to the number of monomer is a straight line not passing through the origin (Figure 12); their equation is written as follows:  $E_{gap}(n) = 2.07 + 4.59/n$  (eV). The intersection of the right with the originally ordered gives the polymer gap energy study [33]. The polymerization of this molecule considerably

reduces this value to a value of the order of 2.07 eV. This result shows that polymer film is a semiconductor material.



**Figure 12.** Variation of gap energy by unit number of the monomer ATT.

#### 4. Conclusions

In conclusion, the results obtained concerning the oxidation of 3-amino-1,2,4-triazole-5-thiol in methanol, in the presence of KOH, reveal the following:

- The cyclic voltammetry recordings show that the oxidation of the monomer exhibits a single oxidation peak corresponding to the oxidation of ATT at 1.15 V
- The voltammograms  $I = f(E)$  and  $I = f(t)$  enabled us to study the properties of the polymeric film as well as the optimal conditions of its formation (effect of applied potential, the pH of electrolytic solution, and solvent nature).
- Electrochemical impedance measurements made it possible to highlight a charge transfer process followed by another purely diffusional one at low frequencies, showing that the synthesized polymer film is a semiconductor.
- Surface analysis by EDX indicates the presence of an organic molecule in the form of a layer covering the surface of the brass electrode
- The gap energy corresponding to poly-ATT is equal to 2.07 eV; this value shows that the polymer film synthesized is a semiconductor in nature.

**Author Contributions:** Original draft preparation, writing—review and editing: M.D. (Mohamed Damej) and N.H.; methodology, formal analysis, H.E. and M.B.; software, validation, writing—review and editing, visualization: M.D. (Mostafa Doubi); methodology, conceptualization, formal analysis, M.A. All authors have read and agreed to the published version of the manuscript.

**Funding:** This research received no external funding.

**Institutional Review Board Statement:** Not applicable.

**Informed Consent Statement:** Not applicable.

**Data Availability Statement:** Not applicable.

**Conflicts of Interest:** The authors declare no conflict of interest.

#### References

1. Bouayadi, H.; Damej, M.; Molhi, A.; Lakbaibi, Z. Electrochemical and theoretical evaluation of thiocarbohydrazide as a brass (60/40) corrosion inhibitor in 3% NaCl solution and effect of temperature on this process. *Int. J. Corros. Scale Inhib.* **2022**, *11*, 1335–1354. [[CrossRef](#)]
2. Rochdi, A.; Kassou, O.; Dkhireche, N.; Touir, R.; El Bakri, M.; Touhami, M.E.; Sfaira, M.; Mernari, B.; Hammouti, B. Inhibitive properties of 2,5-bis(n-methylphenyl)-1,3,4-oxadiazole and biocide on corrosion, biocorrosion and scaling controls of brass in simulated cooling water. *Corros. Sci.* **2014**, *80*, 442–452. [[CrossRef](#)]

3. Gambirasi, A.; Cattarin, S.; Musiani, M.; Vázquez-Gómez, L.; Verlato, E. Electrochimica Acta Direct. *Electrochim. Acta* **2011**, *56*, 8582–8588. [[CrossRef](#)]
4. Kalimuthu, P.; John, S.A. Nanostructured electropolymerized film of 5-amino-2-mercapto-1,3,4-thiadiazole on glassy carbon electrode for the selective determination of l-cysteine. *Electrochem. Commun.* **2009**, *11*, 367–370. [[CrossRef](#)]
5. Kalimuthu, P.; John, S.A. Modification of electrodes with nanostructured functionalized thiadiazole polymer film and its application to the determination of ascorbic acid. *Electrochim. Acta* **2009**, *55*, 183–189. [[CrossRef](#)]
6. Wei, Z.; Zhang, Z.; Wan, M. Formation Mechanism of Self-Assembled Polyaniline Micro/Nanotubes. *Langmuir* **2002**, *18*, 917–921. [[CrossRef](#)]
7. Huang, J.; Virji, S.; Weiller, B.H.; Kaner, R.B. Polyaniline Nanofibers: Facile Synthesis and Chemical Sensors. *J. Am. Chem. Soc.* **2002**, *125*, 314–315. [[CrossRef](#)]
8. An, K.H.; Jeong, S.Y.; Hwang, H.R.; Lee, Y.H. Enhanced sensitivity of a gas sensor incorporating single-walled carbon nanotube–polypyrrole nanocomposites. *Adv. Mater.* **2004**, *16*, 1005–1009. [[CrossRef](#)]
9. Nazari, M.; Agbolaghi, S.; Gheybi, H.; Abbaspoor, S.; Abbasi, F. A focus on the features of polyaniline nanofibres prepared via developing the single crystals of their block copolymers with poly (ethylene glycol). *Bull. Mater. Sci.* **2018**, *41*, 1–11. [[CrossRef](#)]
10. Chebabe, D.; Damej, M.; Dermaj, A.; Oubair, A.; Benassaoui, H.; Erramli, H.; Hajjaji, N.; Srhiri, A. Corrosion Inhibition of Brass in 3% NaCl Solution by Electrosynthesized Poly 4-amino-3-méthyl-1, 2, 4-triazole-5-thione. *Anal. Bioanal. Chem. Res.* **2020**, *7*, 389–401.
11. Trachli, B.; Keddami, M.; Takenouti, H.; Srhiri, A. Protective effect of electropolymerized 2-mercaptobenzimidazole upon copper corrosion. *Prog. Org. Coat.* **2002**, *44*, 17–23. [[CrossRef](#)]
12. Elbakri, M.; Touri, R.; Touhami, M.E.; Srhiri, A.; Benmessaoud, M. Electrosynthesis of adherent poly(3-amino-1,2,4-triazole) films on brass prepared in nonaqueous solvents. *Corros. Sci.* **2008**, *50*, 1538–1545. [[CrossRef](#)]
13. Maynor, B.W.; Filocamo, S.F.; Grinstaff, M.W.; Liu, J.J. Direct-Writing of Polymer Nanostructures: Poly(thiophene) Nanowires on Semiconducting and Insulating Surfaces. *J. Am. Chem. Soc.* **2001**, *124*, 522–523. [[CrossRef](#)] [[PubMed](#)]
14. Bhadra, S.; Singha, N.; Khastgir, D. Effect of aromatic substitution in aniline on the properties of polyaniline. *Eur. Polym. J.* **2008**, *44*, 1763–1770. [[CrossRef](#)]
15. Alvarez, S.; Manolache, S.; Denes, F. Synthesis of polyaniline using horseradish peroxidase immobilized on plasma-functionalized polyethylene surfaces as initiator. *J. Appl. Polym. Sci.* **2003**, *88*, 369–379. [[CrossRef](#)]
16. Chou, C.; Yang, C.; Hsu, C.; Chen, T. Hybrid white-light emitting-LED based on luminescent polyfluorene polymer and quantum dots. *J. Nanosci. Nanotechnol.* **2007**, *7*, 2785–2789. [[CrossRef](#)] [[PubMed](#)]
17. Damej, M.; Chebabe, D.; Benmessaoud, M.; Dermaj, A.; Erramli, H.; Hajjaji, N.; Srhiri, A. Corrosion inhibition of brass in 3% NaCl solution by 3-methyl-1,2,4-triazol-5-thione. *Corros. Eng. Sci. Technol.* **2014**, *50*, 103–107. [[CrossRef](#)]
18. Damej, M.; Benassaoui, H.; Chebabe, D.; Benmessaoud, M.; Erramli, H.; Dermaj, A.; Hajjaji, N.; Srhiri, A. Inhibition effect of 1,2,4-triazole-5-thione derivative on the corrosion of brass in 3% NaCl solution. *J. Mater. Environ. Sci.* **2016**, *7*, 738–745.
19. Damej, M.; Chebabe, D.; About, S.; Erramli, H.; Oubair, A.; Hajjaji, N. Corrosion inhibition of brass 60Cu–40Zn in 3% NaCl solution by 3-amino-1, 2, 4-triazole-5-thiol. *Heliyon* **2020**, *6*, e04026. [[CrossRef](#)]
20. Chebabe, D.; Abdeddine, I.; Bariki, S.; Oubair, A.; About, S.; Damej, M.; Makayssi, A. The Effect of the Chemical Structure of Benzopyridine and Benzimidazole on their Corrosion Inhibiting Action of Ordinary Steel in Acidic Medium. *Anal. Bioanal. Electrochem.* **2019**, *11*, 1701–1715.
21. Damej, M.; Molhi, A.; Tassaoui, K.; El Ibrahim, B.; Akounach, Z.; Addi, A.A.; El Hajjaji, S.; Benmessaoud, M. Experimental and Theoretical Study to Understand the Adsorption Process of p-Anisidine and 4-Nitroaniline for the Dissolution of C38 Carbon Steel in 1M HCl. *ChemistrySelect* **2022**, *7*, e202103192. [[CrossRef](#)]
22. Damej, M.; Hsissou, R.; Berisha, A.; Azgaou, K.; Sadiku, M.; Benmessaoud, M.; Labjar, N.; El Hajjaji, S. New epoxy resin as a corrosion inhibitor for the protection of carbon steel C38 in 1M HCl. Experimental and theoretical studies (DFT, MC, and MD). *J. Mol. Struct.* **2022**, *1254*, 132425. [[CrossRef](#)]
23. About, S.; Zouarhi, M.; Chebabe, D.; Damej, M.; Berisha, A.; Hajjaji, N. Galactomannan as a new bio-sourced corrosion inhibitor for iron in acidic media. *Heliyon* **2020**, *6*, e03574. [[CrossRef](#)]
24. Chafiq, M.; Chaouiki, A.; Damej, M.; Lgaz, H.; Salghi, R.; Ali, I.H.; Benmessaoud, M.; Masroor, S.; Chung, I.M. Bolaamphiphile-class surfactants as corrosion inhibitor model compounds against acid corrosion of mild steel. *J. Mol. Liq.* **2020**, *309*, 113070. [[CrossRef](#)]
25. Molhi, A.; Hsissou, R.; Damej, M.; Berisha, A.; Thaçi, V.; Belafhaili, A.; Benmessaoud, M.; Labjar, N.; El Hajjaji, S. Contribution to the corrosion inhibition of C38 steel in 1 M hydrochloric acid medium by a new epoxy resin PGEPPP. *Int. J. Corros. Scale Inhib.* **2021**, *10*, 399–418. [[CrossRef](#)]
26. Molhi, A.; Hsissou, R.; Damej, M.; Berisha, A.; Bamaarouf, M.; Seydou, M.; Benmessaoud, M.; El Hajjaji, S. Performance of two epoxy compounds against corrosion of C38 steel in 1 M HCl: Electrochemical, thermodynamic and theoretical assessment. *Int. J. Corros. Scale Inhib.* **2021**, *10*, 812–837. [[CrossRef](#)]
27. Benassaoui, H.; Damej, M.; Benassaoui, E.; Dermaj, A.; Erramli, H.; Chebabe, D.; Hajjaji, N.; Srhiri, A. Electrosynthesis and Characterization of Adherent Poly (4-Amino-3 Methyl-1,2,4-Triazole-5-Thione) Films on B66 Bronze Electrode in Methanol. *Port. Electrochim. Acta* **2020**, *38*, 299–312. [[CrossRef](#)]

28. Aghazadeh, M. Cathodic electrochemical deposition of nanostructured metal oxides/hydroxides and their composites for supercapacitor applications: A review. *Anal. Bioanal. Electrochem.* **2019**, *11*, 211–266.
29. Kiya, Y.; Henderson, J.C.; Abruña, H.D. 4-Amino-4H-1,2,4-triazole-3,5-dithiol. *J. Electrochem. Soc.* **2007**, *154*, A844. [[CrossRef](#)]
30. Arbizzani, C.; Mastragostino, M.; Meneghello, L. Polymer-based redox supercapacitors: A comparative study. *Electrochim. Acta* **1996**, *41*, 21–26. [[CrossRef](#)]
31. Vorotyntsev, M.A.; Badiali, J.P.; Inzelt, G. Electrochemical impedance spectroscopy of thin films with two mobile charge carriers: Effects of the interfacial charging. *J. Electroanal. Chem.* **1999**, *472*, 7–19. [[CrossRef](#)]
32. Garcia-Belmonte, G.; Fabregat-Santiago, F.; Bisquert, J.; Yamashita, M.; Pereira, E.C.; Castro-Garcia, S. Frequency dispersion in electrochromic devices and conducting polymer electrodes: A generalized transmission line approach. *Ionics* **1999**, *5*, 44–51. [[CrossRef](#)]
33. Ayachi, S.; Ghomrasni, S.; Bouachrine, M.; Hamidi, M.; Alimi, K. Structure–property relationships of soluble poly(2,5-dibutoxyethoxy-1,4-phenylene-alt-2,5-thienylene) (PBUPT) for organic-optoelectronic devices. *J. Mol. Struct.* **2013**, *1036*, 7–18. [[CrossRef](#)]